Photoluminescence properties of Mn^{4+}-activated Li$_2$ZnSn$_2$O$_6$ red phosphors

Byoung Su Choi[a], Dong Hwa Lee[b], Jeong Ho Ryu[c] and Hyun Cho[b,*]

[a]Department of Nano Fusion Technology, Pusan National University, Gyeongnam 50463, Korea
[b]Department of Nanomechatronics Engineering, Pusan National University, Busan 46241, Korea
[c]Department of Materials Science and Engineering, Korea National University of Transportation, Chungbuk 27469, Korea

The Mn^{4+}-activated Li$_2$ZnSn$_2$O$_6$ (LZSO:Mn^{4+}) red phosphors were synthesized by the solid-state reaction at temperatures of 1100-1400 ^{o}C in air. The synthesized LZSO:Mn^{4+} phosphors were confirmed to have a single hexagonal LZSO phase without the presence of any secondary phase formed by the Mn^{4+} addition. With near UV and blue excitation, the LZSO:Mn^{4+} phosphors exhibited a double band deep-red emission peaked at ~658 nm and ~673 nm due to the ^{2}E → ^{4}A$_2$ transition of Mn^{4+} ion. PL emission intensity showed a strong dependence on the Mn^{4+} doping concentration and the 0.3 mol% Mn^{4+}-doped LZSO phosphor produced the strongest PL emission intensity. Photoluminescence emission intensity was also found to be dependent on the calcination temperature and the optimal calcination temperature for the LZSO:Mn^{4+} phosphors was determined to be 1200 ^{o}C. Dynamic light scattering (DLS) and field-effect scanning electron microscopy (FE-SEM) analysis revealed that the 0.3 mol% Mn^{4+}-doped LZSO phosphor particles have an irregularly round shape and an average particle size of ~1.46 μm.

Key words: Li$_2$ZnSn$_2$O$_6$:xMn^{4+} phosphors, Solid-state reaction, Deep red emission, Photoluminescence properties.

Introduction

Recently white light-emitting diodes (w-LEDs) has become an essential component for display lighting and illumination systems because of their high efficiency, low power consumption and long lifetime. A world-wide commercial approach to achieve white light emission is to combine a yellow-emitting YAG:Ce^{3+} phosphor and a III-nitride semiconductor-based blue emitting LED chip as the excitation source. However this type of w-LEDs exhibit a cold white light with a poor color rendering index (CRI) and high color temperature due to lack of a red color component in luminescence and this limits their applications in general illumination systems. In order to realize the w-LEDs emitting a warm white light, it is important to develop a new red-emitting phosphor [1-5].

To date, Mn^{4+} and Eu^{2+} ions are the most frequently reported activator metal ions among many studies on red phosphors. Of these two ions, Mn^{4+} ion is more attractive as the activator for red phosphors. Mn^{4+} ion has incompletely filled 3d shell and locates in the octahedral sites in the lattice. The Mn^{4+}-doped luminescent materials generally show typical optical properties consisted of broad excitation band over the range of 200-500 nm due to the ^{4}A$_2$ → (^{4}T$_1$, ^{2}T$_2$, and ^{4}T$_2$) transitions and red to near-infrared emission within 600-780 nm due to the ^{2}E → ^{4}A$_2$ while the Eu^{2+}-doped red phosphors exhibit sharp absorption peaks in UV and blue region. Furthermore, non-rare earth Mn^{4+} ion has the advantage of being lower in cost compared to the rare earth Eu^{2+} and can be efficiently activated in various host materials such as aluminates [6-8], titanates [9-11], and fluorides [12-14], and so on. Owing to these advantages, intensive research work has been conducted recently on the red phosphors using the Mn^{4+} ion as activator.

In this work, we report non-rare earth Mn^{4+}-activated Li$_2$ZnSn$_2$O$_6$ (LZSO) red phosphors for the application in the w-LEDs. The LZSO:Mn^{4+} red-emitting phosphors with Mn^{4+} doping concentration of 0.1-0.9 mol% were synthesized via a solid-state reaction route and the effects of solid-state reaction temperature and doping concentration on their photoluminescence properties were studied.

Experimental

Mn^{4+}-activated Li$_2$ZnSn$_2$O$_6$ (LZSO:Mn^{4+}) phosphors were synthesized by the solid-state reaction method. High purity Li$_2$CO$_3$ (LTS Research Laboratories, Inc., 99,995%), ZnO (Alfa Aesar, 99.99%), SnO$_2$ (LTS Research Laboratories, Inc., 99,99%), and MnCO$_3$ (High Purity Chemicals, 99.9%) were used as starting materials. Doping concentration of Mn^{4+} was varied from 0.1 to 0.9 mol% with respect to Sn^{4+}. Stoichiometric mixtures of Li$_2$CO$_3$, ZnO, SnO$_2$ and

*Corresponding author:
Tel : +82-51-510-6113
Fax: +82-51-514-2358
E-mail: hyuncho@pusan.ac.kr

MnCO$_3$ powders were weighed and homogeneously mixed by ball-milling, and then were calcined at temperatures of 1100 to 1400 °C for 10 h in air. After calcination, the phosphor samples were mildly ground before photoluminescence measurements. The crystalline phase of the synthesized phosphor powders was identified by X-ray diffraction (XRD) analysis with Cu-Kα radiation operated at 40 kV and 30 mA (Panalytical Empyrean Series 2). The photoluminescence emission and excitation spectra were collected at room temperature using a Fluorescence spectrometer (FluoroMate FS-2, SCINCO) in the range of 400-700 nm and 360-500 nm, respectively. Particle size distribution and average particle size were measured by particle size analyzer (PSA, Malvern Zeta Sizer Nano ZS), and morphology of the synthesized phosphors were observed by scanning electron microscopy (SEM, Hitachi S-4700).

Results and Discussion

Fig. 1 shows the XRD patterns of the prepared Li$_2$ZnSn$_{(2-x)}$O$_6$:xMn^{4+} (x = 0.1, 0.3, 0.5, 0.7 and 0.9 mol%) phosphors calcined at 1200 °C for 10 h in air. It is clear that the synthesized LZSO:Mn^{4+} phosphors show the characteristic diffraction patterns which is consistent with the hexagonal phase Li$_2$ZnSn$_2$O$_6$ (Joint Committee on Powder Diffraction Standards No. 22-425). This indicates that all of the LZSO:Mn^{4+} phosphors with different Mn^{4+} doping concentration are synthesized in a single hexagonal phase structure without formation of secondary phases by Mn^{4+} addition into LZSO. The doped Mn^{4+} ion replaces Sn^{4+} ion in [SnO$_6$] octahedron in host LZSO lattice due to similar ionic radius and bond coordination characteristics (Sn^{4+}: ~0.69 Å, six-coordinated and Mn^{4+}: ~0.54 Å, six-coordinated) [15]. It is also found that the temperature of 1200 °C is high enough to complete the solid state reaction to form LZSO since no evident
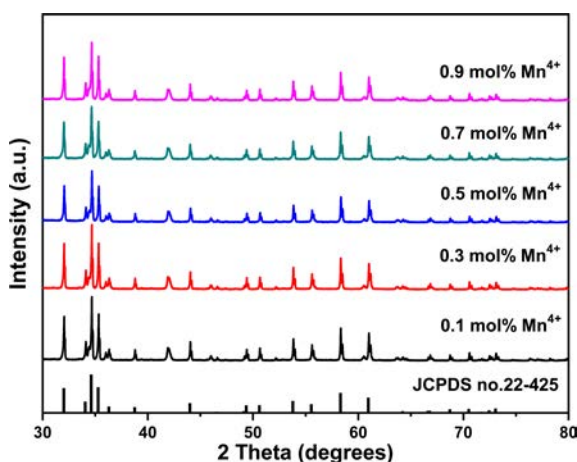
peaks of the unreacted starting materials are detected in the XRD analysis.

Fig. 2 shows the photoluminescence (PL) excitation spectra in the range of 400-550 nm (λ_{em} = 658 nm) (Fig. 2(a)) and PL emission spectra of the synthesized LZSO:Mn^{4+} phosphors with variation of Mn^{4+} doping concentration (Fig. 2(b)) at room temperature. The PL excitation band in the range of 430-530 nm is attributed to the $^4A_2 \rightarrow ^4T_2$ transition of Mn^{4+} ion at ~469 nm.[16, 17] The LZSO:Mn^{4+} phosphors excited by 469 nm pumping sources can emit deep-red light and their PL spectra are consisted of a double band red emission peaked at ~658 nm and ~673 nm, respectively. These two PL peaks are attributed to the lattice vibration modes of the transition $^2E \rightarrow ^4A_2$ for the 3d^3 electrons of Mn^{4+} ion in [MnO$_6$] octahedral symmetry [18,19].

The PL properties of the LZSO:Mn^{4+} phosphors show a strong dependence on the Mn^{4+} doping concentration. Fig. 3 shows the effect of the Mn^{4+} doping concentration on the PL emission peak intensity with excitation of 365 and 469 nm, respectively. The PL emission intensity of the prepared LZSO:Mn^{4+} phosphors initially increases as the Mn^{4+} doping concentration increases and reaches a maximum at 0.3 mol%, and then decreases at the concentration beyond 0.3 mol% due to the concentration quenching effect. This is most likely due to the probability of the energy transfer from the Mn^{4+} ions at higher levels of 3d to those at the lower levels of 3d increases with the
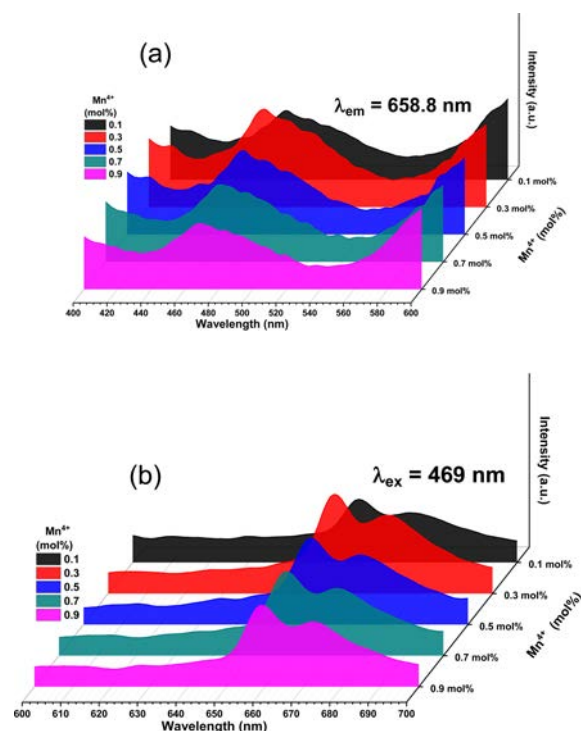

Fig. 2. (a) Photoluminescence excitation (λ_{em} = 658.8 nm) and (b) photoluminescence emission (λ_{ex} = 469 nm) spectra of the LZSO:Mn^{4+} phosphors with different Mn^{4+} doping concentration prepared at 1200 °C in air.
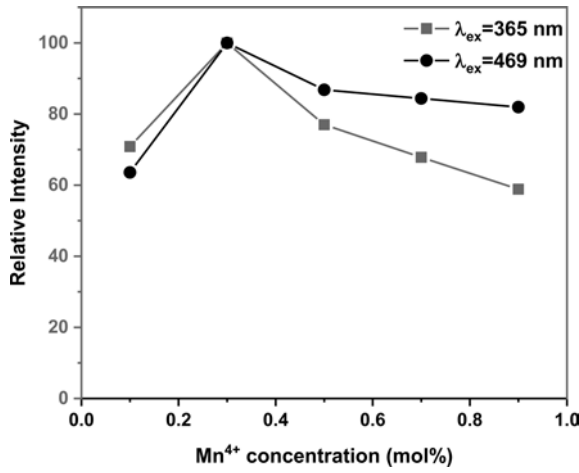

Fig. 1. X-ray diffraction patterns of the LZSO:Mn^{4+} phosphors with different Mn^{4+} doping concentration prepared at 1200 °C in air.

Fig. 3. Relative photoluminescence emission intensity of the LZSO:Mn^{4+} phosphor as a function of Mn^{4+} doping concentration.

Fig. 5. A SEM micrograph and particle size distribution profile of the 0.3 mol% Mn^{4+}-doped LZSO phosphor prepared at 1200 °C in air.
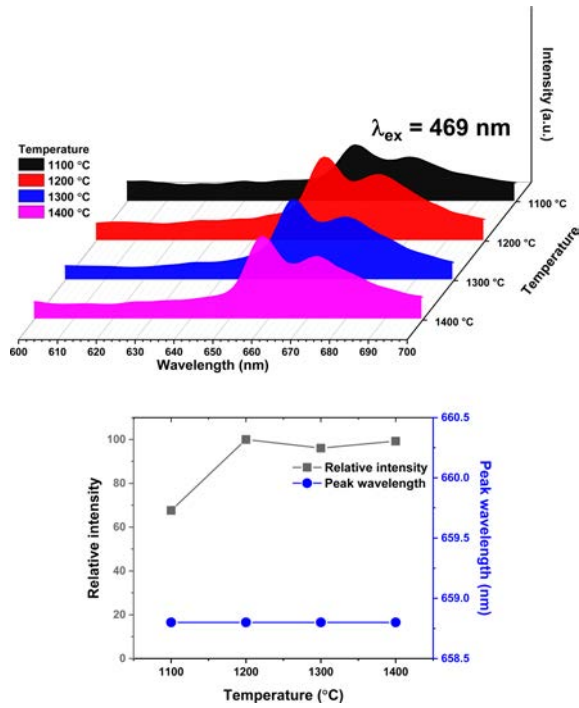

Fig. 4. Photoluminescence emission spectra ($\lambda_{ex} = 469$ nm) and relative PL emission intensity of the 0.3 mol% Mn^{4+}-doped LZSO phosphor prepared at temperatures of 1100-1400 °C in air.

Mn^{4+}-doped LZSO phosphor synthesized at the calcination temperature of 1200 °C shows the strongest PL emission intensity due to the combined effect of stable host lattice structure and strong crystal field.

Fig. 5 shows the morphology and particle size distribution profile of the LZSO:Mn^{4+} phosphor examined by SEM and dynamic light scattering (DLS). This LZSO:Mn^{4+} phosphor was synthesized at a Mn^{4+} doping concentration of 0.3 mol% and a calcination temperature of 1200 °C where the strongest PL emission peak intensity was obtained. The synthesized 0.3 mol% Mn^{4+} doped LZSO phosphor is found to have an average particle size of ~1.46 μm with a narrow distribution profile in the range of ~1.0-2.1 μm and each particle has an irregularly round shape. It is known that the shape of the phosphor particles affects the performance of the phosphor. Considering the size uniformity and particle shape of the LZSO:Mn^{4+} phosphor synthesized in this study, the scattering effect on the PL efficiency is expected to be insignificant.

increase of the Mn^{4+} doping concentration. The optimal Mn^{4+} doping concentration is found to be 0.3 mol%.

The effect of calcination temperature on the PL properties of the 0.3 mol% Mn^{4+}-doped LZSO phosphor ($\lambda_{ex} = 469$ nm) is shown in Fig. 4. It can be seen that all of the 0.3 mol% Mn^{4+}-doped LZSO phosphors prepared at different calcination temperatures exhibit almost identical PL spectral shape and peak wavelength. This suggests that the activator Mn^{4+} ion only replaces for one octahedral site, i.e. Sn^{4+} ion in [SnO$_6$] octahedron, in the host LZSO lattice and is affected by the same crystal field under these conditions. The 0.3 mol%
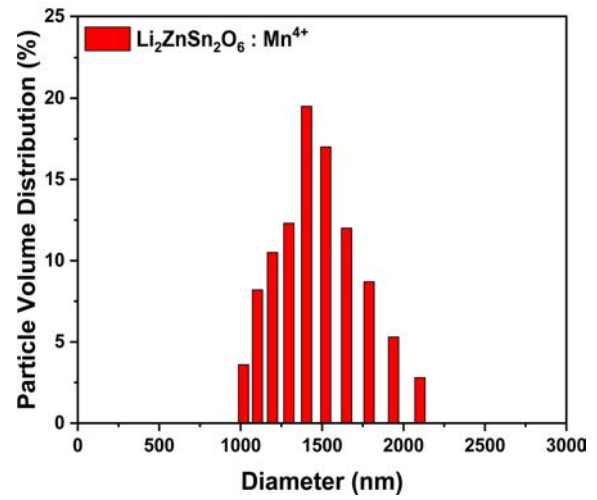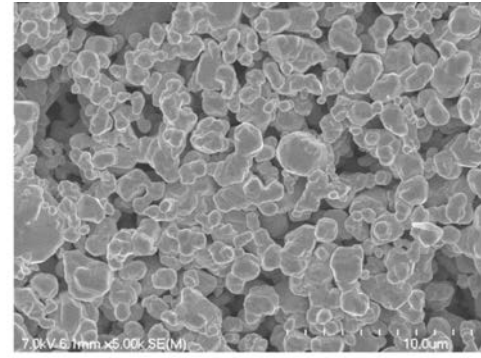
Conclusions

The Mn^{4+}-activated LZSO red phosphors were synthesized by a solid-state reaction method in air and the effects of Mn^{4+} doping concentration and calcination temperature on their photoluminescence properties have been examined. XRD analysis confirmed that the LZSO:Mn^{4+} phosphors with Mn^{4+} doping concentration of 0.1-0.9 mol% have a single hexagonal phase structure and the doped Mn^{4+} ion replaces for the Sn^{4+} ion in the host LZSO lattice. The LZSO:Mn^{4+} phosphor showed the PL excitation peak at ~469 nm attributed to the $^4A_2 \rightarrow {}^4T_2$ transition of Mn^{4+} ion and exhibited deep-red emission consisted of a double band peaked at ~658 nm and ~673 nm due to the $^2E \rightarrow {}^4A_2$ transition of Mn^{4+} ion under near UV and blue excitation. The optimal Mn^{4+} doping concentration and calcination temperature for the LZSO:Mn^{4+} phosphor with high efficiency were found to be 0.3 mol% and 1200 °C, respectively. The results has demonstrated that the LZSO:Mn^{4+} system has a good potential as a red phosphor for white LED using near UV or blue LEDs as the excitation source.

References

1. R. Cao, M. Peng, and J. Qiu, Opt. Exp. 20 (2012) A977-A983.
2. K. Takahashi, N. Hirosaki, R. Xie, M. Harada, K. Yoshimaura, and Y. Tomomura, Appl. Phys. Lett. 91 (2007) 091923 (091923-1-091923-3).
3. Y. Hu, W. Zhuang, H. Ye, S. Zhang, Y. Fang, and X. Huang, J. Lumin. 111 (2005) 139-145.
4. S. Nakamura, and G. Fasol, in "The Blue Laser Diode: GaN Based Light Emitters and Lasers" (Springer, Berlin, 1996), p. 1-24.
5. Q. Sai, C. Xia, H. Rao, X. Xu, G. Zhou, and P. Xu, J. Lumin. 131 (2011) 2359-2364.
6. T. Murate, T. Tanoue, M. Iwasaki, K. Morinaga, and T. Hase, J. Luminescence 114 (2005) 207-212.
7. R. Cao, F. Zhang, C. Cao, X.Yu, A. Liang, S. Guo, and H. Xue, Opt. Mater. 38 (2014) 53-56.
8. L. Chen, X. Deng, E. Zhao, X. Chen, S. Xue, W. Zhang, S. Chen, Z. Zhao, W. Zhang, and T. Chan, J. Alloy Compd. 613 (2014) 22905-22913.
9. K. Seki, S. Kamei, K. Uematsu, T. Ishigaki, K. Toda, and M. Sato, J. Ceram. Proc. Res. 14 (2013) s67-s70.
10. Y. Lin, Y. Hu, H. Wu, H. Duan, L. Chen, Y. Yu, G. Ju, Z. Mu, and M. He, Chem. Eng. J. 288 (2016) 596-607.
11. Y. Takeda, H. Kato, M. Kabayashi, H. Kobayashi, and M. Kakihana, Chem. Lett. 44 (2015) 1541-1543.
12. L.L. Wei, C.C. Lin, Y.Y. Wang, M.H. Fang, H. Jiao, and R.S. Liu, ACS Appl. Mater. Interfaces 7 (2015) 10656-10659.
13. Q. Zhou, Y. Zhou, Y. Liu, Z. Wang, G. Chen, J. Peng, J. Yan, and M. Wu, J. Mater. Chem. C 3 (2015) 9615-9619.
14. Y. Jin, M.H. Fang, M. Grinberg, S. Mahlik, T. Lesniewski, M.G. Brik, G.Y. Luo, J.G. Lin, and R.S. Liu, ACS Appl. Mater. Interfaces 8 (2016) 11194-11203.
15. R.D. Shannon, Acta Crystallogr. A 32 (1976) 751-767.
16. M.H. Du, J. Mater. Chem. C 2 (2014) 2475-2481.
17. R. Cao, X. Liu, K. Bai, T. Chen, S. Guo, Z. Hu, F. Xiao, and Z. Luo, J. Luminescence 197 (2018) 169-174.
18. R. Cao, W. Luo, H. Xu, Z. Luo, Q. Hu, T. Fu, and D. Peng, Opt. Mater. 53 (2016) 169-173.
19. W. Shen, Y. Liu, and Z. Wang, Mater. Lett. 161 (2015) 140-143.